Mimicking the HDS Activity of Ruthenium-Based Catalysts 2: The Hydrogenation of Benzo[*b*]thiophene to 2,3-Dihydrobenzo[*b*]thiophene

Claudio Bianchini,*,† Andrea Meli,† Simonetta Moneti,† Werner Oberhauser,† Francesco Vizza,† Verónica Herrera,‡ Alberto Fuentes,‡ and Roberto A. Sánchez-Delgado*,‡

Contribution from the Istituto per lo Studio della Stereochimica ed Energetica dei Composti di Coordinazione, ISSECC-CNR, 50132 Firenze, Italy, and Instituto Venezolano de Investigaciones Científicas, IVIC, Caracas 1020-A, Venezuela

Received September 9, 1998

Abstract: The ruthenium(II) tris-acetonitrile complex [(triphos)Ru(MeCN)$_3$]BPh$_4$ (**1**) is an extremely efficient catalyst precursor for the regioselective hydrogenation of benzo[*b*]thiophene (BT) to 2,3-dihydrobenzo[*b*]-thiophene (DHBT) in homogeneous phase under mild reaction conditions (THF, 40−100 °C, 1−30 bar H_2) [triphos = MeC(CH$_2$PPh$_2$)$_3$]. At 30 bar of H_2 and 100 °C, BT is converted to DHBT with an average rate of 500 mol of product (mol of cat)$^{-1}$ h^{-1}. During the catalytic reactions with $PH_2 > 5$ bar, the acetonitrile ligands in **1** are transformed into a mixture of NHEt$_2$, NEt$_3$, and NH_3, while the termination ruthenium products are the monohydrido complexes [(triphos)Ru(H)(NH$_3$)$_2$]BPh$_4$, [(triphos)Ru(H)(NH$_3$)(NH$_2$Et)]BPh$_4$, and [(triphos)-Ru(H)(NH$_3$)(η^1-*S*-DHBT)]BPh$_4$. Below 5 bar of H_2, no hydrogenation of MeCN occurs and all of the ruthenium is recovered as [(triphos)Ru(H)(NCMe)(η^1-*S*-DHBT)]BPh$_4$. All of these Ru(II) hydrido complexes catalyze the hydrogenation of BT to DHBT as efficiently as **1**. The substitution of D_2 for H_2 in a catalytic reaction shows that BT is selectively *cis*-deuterated to DHBT-d_2 with no deuterium enrichment in either the unreacted BT or the arene ring of DHBT. Water in the reaction mixture decreases the hydrogenation rate of BT due to the formation of the μ-OH and acetate Ru(II) complexes [(triphos)Ru(μ-OH)$_3$Ru(triphos)]BPh$_4$ and [(triphos)Ru(O$_2$CCH$_3$)(OH$_2$)]BPh$_4$, which are catalytically inactive. The acetate complex is suggested to form via hydration of a MeCN ligand in the catalyst precursor. Catalytic runs at 30 and 2 bar of H_2 were studied in situ by high-pressure NMR spectroscopy. The kinetics of the hydrogenation of BT in the presence of **1** were studied by gas adsorption techniques at different catalyst, substrate, and dihydrogen concentrations and at different temperatures. The kinetic data together with all of the other evidence accumulated allowed us to deduce a catalytic cycle in which the reversible dissociation of the thioether product from the metal center in the catalyst [(triphos)RuH]$^+$ is a rate-limiting step. A comparison of the hydrogenation reactions of BT catalyzed by either the Ru(II) 14e$^-$ fragment [(triphos)RuH]$^+$ or the Ru(0) 16e$^-$ fragment [(triphos)RuH]$^-$ has provided some clues to unravel a number of mechanistic aspects of the HDS of thiophenes over single-component catalysts. In particular, the occurrence of either hydrogenation to thioether or hydrogenolysis to thiol has been related with the metal basicity.

Introduction

During the hydrotreating of petroleum feedstocks in refineries, sulfur compounds, among which the thiophenes are quite abundant and most difficult to degrade, are converted to hydrocarbons and H_2S via the hydrodesulfurization process (HDS).[1] In this procedure, fossil fuels are hydrogenated at high temperature over heterogeneous catalysts. Conventional catalysts are a combination of molybdenum (or tungsten) (metal *component*) and cobalt (metal *promoter*) where Mo (W) and Co exist primarily as binary sulfides. Various late transition metals can act as *promoters* (Ni, Ru, Pt, Pd, Rh, Ir, Os).[1]

In recent years, numerous studies of the variations of the HDS activity exhibited by transition metal sulfides as a function of the position of the metal in the Periodic Table have appeared in the literature.[2] Irrespective of the method employed to assess the periodic trends, either volcano-type or monotonic dependences of the HDS activity have been obtained in which ruthenium is almost invariably located on the top of the curve.[2]

The chemical reasons for the excellent HDS activity of RuS_2 are still a matter of intense debate and also contrast sharply

† ISSECC-CNR.

‡ IVIC.

(1) (a) Topsøe, H.; Clausen, B. S.; Massoth, F. E. *Hydrotreating Catalysis*; Springer-Verlag: Berlin, Germany, 1996. (b) Scherzer, J.; Gruia, A. J. *Hydrocracking Science and Technology*; Marcel Dekker: New York, 1996. (c) van den Berg, J. P.; Lucien, J. P.; Germaine, G.; Thielemans, G. L. B. *Fuel Process. Technol.* **1993**, *35*, 119. (d) Gates B. C. *Catalytic Chemistry*; John Wiley: New York, 1992; Chapter 5, p 390. (e) Prins, R.; de Beer, V. H. J.; Somorjai, G. A. *Catal. Rev.−Sci. Eng.* **1989**, *31*, 1.

(2) (a) Harris, S.; Chianelli, R. R. In *Theoretical Aspects of Heterogeneous Catalysis*; Moffat, J. B., Ed.; van Nostrand Reinhold Catalysis Series, van Nostrand Reinhold: New York, 1990; p 206. (b) Chianelli, R. R. *Catal. Rev.−Sci. Eng.* **1984**, *26*, 361. (c) Pecoraro, T. A.; Chianelli, R. R. *J. Catal.* **1981**, *67*, 430. (d) Hensen, E. J. M.; de Beer, V. H. J.; van Santen, R. A. In *Transition Metal Sulphides*; Weber, T., Prins, R., van Santen, R. A., Eds.; Kluwer Academic Publishers: Dordrecht, The Netherlands, 1998; p 169. (e) Topsøe, H.; Clausen, B. S.; Topsøe, N.-J.; Nørskov, J. K.; Ovesen, C. V.; Jacobsen, C. J. H. *Bull. Soc. Chim. Belg.* **1995**, *104*, 283. (f) Topsøe, H.; Clausen, B. S.; Topsøe, N.-J.; Hyldoft, J.; Nørskov, J. K. *Prepr.−Am. Chem. Soc., Div. Pet. Chem.* **1993**, *38*, 638. (g) Nørskov, J. K.; Clausen, B. S.; Topsøe, H. *Catal. Lett.* **1992**, *13*, 1. (h) Tan, A.; Harris, S. *Inorg. Chem.* **1998**, *37*, 2215.

10.1021/ja983224e CCC: $18.00
Published on Web 07/16/1999

with the scarce use of Ru-promoted catalysts in actual hydrotreating reactors. Chianelli and co-workers have related the high HDS activity of RuS_2 to an optimum metal−sulfur bond strength,[2a−c] a concept developed later by van Santen who has proposed that the reaction rate is slow to the left of the maximum activity due to high metal−sulfur interaction energies, while to the right of the maximum, the interaction energy is too low, leading to unstable intermediates.[2d] Following a similar reasoning, Nørskov and Tøpsoe have suggested that the most active metal sulfides are just those with the lowest sulfur-binding energy (Ru, Os, Rh, Ir).[2e−g] According to this interpretation, the number of sulfur vacancies may be the key factor controlling the activity trend. More recently, Tan and Harris, by using band structure calculations,[2h] have proposed that the nearly complete localization of electron density in the metal t_{2g} orbitals in RuS_2 may account for the high HDS activity. Calculations on the (210) and (111) surfaces of RuS_2 have clearly shown the existence of a correlation between the electronic properties of 5-, 4-, and 3-coordinate surface Ru atoms and the type of activation undergone by the adsorbed thiophene. In particular, the activation can be followed by the key step of C−S bond cleavage only when the metal center, eventually 3-coordinate, is made electron-rich by the reducing atmosphere of the high pressure of H_2 used in HDS as well as by electron transfer from bulk Ru atoms.

On the basis of the model reactor studies and the fact the Ru−Mo−S interaction phase[3] is similar to the largely employed Co−Mo−S phase,[1a] ruthenium might have indeed a great potential as HDS *promoter* once the factors that cause the deactivation of the catalysts in actual refining conditions will be understood and hopefully bypassed. In this perspective, homogeneous modeling studies applying soluble ruthenium complexes might contribute to elucidate the mechanisms through which ruthenium either catalyzes the hydrogenation, hydrogenolysis, and desulfurization of the thiophenes or is deactivated during the process.[4]

Despite the relatively high number of the model studies involving ruthenium compounds,[4,5] detailed studies of their catalytic properties in the hydrogenation of thiophenic substrates have not yet been reported.[6] This scarcity of experimental data has motivated our decision to investigate the catalytic activity of different ruthenium complexes in the hydrogenation of thiophenes varying the reaction parameters as systematically as possible.

Scheme 1

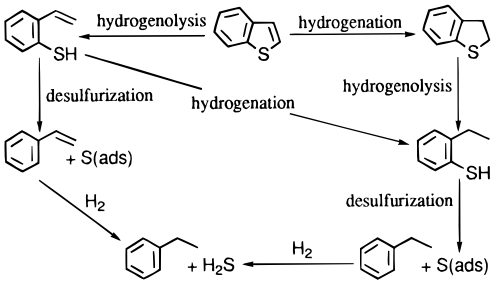

In a previous paper, we have described the first example of homogeneous and chemoselective hydrogenolysis of benzo[*b*]-thiophene (BT) to 2-ethylthiophenol (ETP) effectively catalyzed by the Ru(0) 16e$^-$ fragment [(triphos)RuH]$^-$ obtained by the thermolysis of the ruthenate complex K[(triphos)RuH_3] [(triphos = $MeC(CH_2PPh_2)_3$].[7] Herein we report a detailed account (comprising high-pressure NMR studies in sapphire tubes, reactor studies at elevated pressure of H_2, deuterium-labeling experiments, and kinetic studies) of the regioselective hydrogenation of BT to the cyclic thioether 2,3-dihydrobenzo[*b*]-thiophene (DHBT) catalyzed by the Ru(II) 14e$^-$ fragment [(triphos)RuH]$^+$ obtained by hydrogenation of the precursor [(triphos)Ru$(MeCN)_3$]$(BPh_4)_2$ (**1**) (eq 1).

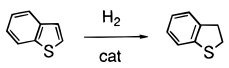

(1)

The hydrogenation to thioethers and the hydrogenolysis to thiols represent the preliminary and mechanistically crucial steps of the HDS of BT as well as any other thiophenic substrate (see Scheme 1 for BT). The parallel, alternative, or competitive occurrence of the hydrogenation and hydrogenolysis paths under actual HDS conditions constitutes a heated debate among heterogeneous and organometallic chemists.[1,4] Indeed, understanding this mechanistic aspect, strictly related to the electronic nature of the surface metal atoms and to the preparation and pretreatment of the catalytic material, is of crucial importance for the development of catalysts specifically tailored for the HDS of thiophenes via the energetically favored hydrogenolysis mechanism. Within this context, the present study may provide a key to unravel the hydrogenation/hydrogenolysis dichotomy through a comparison of the reactivity of the isostructural but not isolectronic Ru catalysts [(triphos)RuH]$^-$ and [(triphos)-RuH]$^+$.

Experimental Section

1. General Information. All reactions and manipulations, except as stated otherwise, were routinely performed under a nitrogen atmosphere by using standard Schlenk techniques. Reactions under a controlled pressure of hydrogen were performed with a stainless steel Parr 4565 reactor (100 mL) equipped with a Parr 4842 temperature and pressure controller. The ruthenium colloid $Ru[N(octyl)_4Br]_n$[8] (Ru, 68.3%) and the complexes [(triphos)Ru$(NCMe)_3$]$(BPh_4)_2$ (**1**) and

(3) (a) Xiao, F.-S.; Xin, Q.; Guo, X.-X. *Appl. Catal., A* **1993**, *95*, 21. (b) Geantet, C.; Göbölös, S.; De Los Reyes, J. A.; Cottenot, M.; Vrinat, M.; Breysse, M. *Catal. Today* **1991**, *10*, 665. (c) Mitchell, P. C. H.; Scott, C. E. *Bull. Soc. Chim. Belg.* **1984**, *93*, 619.

(4) (a) Bianchini, C.; Meli, A. In *Aqueous-Phase Organometallic Catalysis − Concepts and Applications*; Cornils, B., Herrmann, W. A., Eds.; VCH: Weinheim, Germany, 1998; p 477. (b) Bianchini, C.; Meli, A. *Acc. Chem. Res.* **1998**, *31*, 109. (c) Bianchini, C.; Meli, A. In *Applied Homogeneous Catalysis with Organometallic Compounds*; Cornils, B., Herrmann, W. A., Eds.; VCH: Weinheim, Germany, 1996; Vol. 2, p 969. (d) Bianchini, C.; Meli, A. *J. Chem. Soc., Dalton Trans.* **1996**, 801. (e) Angelici, R. J. *Bull. Soc. Chim. Belg.* **1995**, *104*, 265. (f) Angelici, R. J. In *Encyclopedia of Inorganic Chemistry*; King, R. B., Ed.; John Wiley: New York, 1994; Vol. 3, p 1433. (g) Sánchez-Delgado, R. A. *J. Mol. Catal.* **1994**, *86*, 287. (h) Rauchfuss, T. B. *Prog. Inorg. Chem.* **1991**, *39*, 259. (i) Angelici, R. J. *Coord. Chem. Rev.* **1990**, *105*, 61. (j) Angelici, R. J. *Acc. Chem. Res.* **1988**, *21*, 387.

(5) (a) Bianchini, C.; Masi, D.; Meli, A.; Peruzzini, M.; Vizza, F.; Zanobini, F. *Organometallics* **1998**, *17*, 2495. (b) Bianchini, C.; Casares, J. A.; Osman, R.; Pattison, D. I.; Peruzzini, M.; Perutz, R. N.; Zanobini, F. *Organometallics* **1997**, *16*, 4611. (c) Feng, Q.; Rauchfuss, T. B.; Wilson, S. R. *Organometallics* **1995**, *14*, 2923. (d) Dailey, K. M.; Rauchfuss, T. B.; Rheingold, A. L.; Yap, G. P. A. *J. Am. Chem. Soc.* **1995**, *117*, 6396. (e) Arce, J. A.; De Sanctis, Y.; Karam, A.; Deeming, J. A. *Angew. Chem., Int. Ed. Engl.* **1994**, *33*, 1381. (f) Luo, S.; Rauchfuss, T. B.; Gan, Z. *J. Am. Chem. Soc.* **1993**, *115*, 4943. (g) Krautscheid, H.; Feng, Q.; Rauchfuss, T. B. *Organometallics* **1993**, *12*, 3273. (h) Hachgenei, J. W.; Angelici, R. J. *Angew. Chem., Int. Ed. Engl.* **1987**, *26*, 909. (i) Hachgenei, J. W.; Angelici, R. J. *J. Organomet. Chem.* **1988**, *355*, 359.

(6) (a) Páez, D. E.; Andriollo, A.; Sánchez-Delgado, R.; Valencia, N.; López-Linares, F.; Galiasso, R. E. INTEVEP SA; U.S. Patent 5753584, May 19, 1998. (b) Sánchez-Delgado, R. A.; González, E. *Polyhedron* **1989**, *8*, 1431. (c) Fish, R. H.; Tan, J. L.; Thormodsen, A. D. *Organometallics* **1985**, *4*, 1743.

(7) Bianchini, C.; Meli, A.; Moneti, S.; Vizza, F. *Organometallics* **1998**, *17*, 2636.

(8) Bönnemann, H.; Brijoux, W.; Brinkmann, R.; Dinjus, E.; Jouβen, T.; Korall, B. *Angew. Chem., Int. Ed. Engl.* **1991**, *30*, 1312.

Table 1. Hydrogenation of Benzo[*b*]thiophene Catalyzed by $[(Triphos)Ru(NCMe)_3](BPh_4)_2$ (1)[a]

entry	BT (mmol)	PH_2 (bar)	time (h)	T (°C)	conv. (%)	DHBT rate[b]
1	21.5	30	1	100	100.0	500.0
2[c]	21.5	30	1	100	100.0	500.0
3	4.3	30	1	60	93.1	93.1
4	4.3	30	1	40	46.0	46.0
5	4.3	30	5	40	90.2	18.0
6	4.3	15	5	40	78.9	15.8
7	4.3	10	5	40	76.3	15.3
8	4.3	5	5	40	65.8	13.2
9	4.3	2	5	40	53.6	10.7
10	4.3	1.5	5	40	36.3	7.2
11	4.3	1	5	40	15.3	3.1

[a] Reaction conditions: catalyst (0.043 mmol), THF (30 mL), stirring (750 rpm). [b] Average rate expressed as moles of DHBT per mol of catalyst per hour. [c] THF (28.5 mL) + H_2O (1.5 mL).

$[(triphos)Ru(H)(NCMe)_2]BPh_4$ (**2**) were prepared as previously described.[7] All of the isolated metal complexes were collected on sintered-glass frits and washed with appropriate solvents before being dried under a stream of nitrogen. Tetrahydrofuran (THF) and THF-d_8 were purified by distillation under nitrogen from $LiAlH_4$. MeCN was distilled from CaH_2. Benzo[*b*]thiophene (99%, Aldrich) was sublimed prior to use. Poly(vinylpyrrolidone) K25 (average M_W 29 000) was purchased from Aldrich and used without further purification. All of the other reagents and chemicals were reagent grade and used as received from commercial suppliers. ^1H (200.13 MHz), $^{13}C\{^1H\}$ (50.32 MHz), and $^{31}P\{^1H\}$ (81.01 MHz) NMR spectra were obtained on a Bruker ACP 200 spectrometer. All chemical shifts are reported in parts per million (δ) relative to tetramethylsilane, referenced to the chemical shifts of residual solvent resonances (^1H, ^{13}C) or 85% H_3PO_4 (^{31}P). ^1H NMR experiments on 2,3-dihydrobenzo[*b*]thiophene-d_2 were conducted on a Bruker AMX 600 spectrometer (600.13 MHz). The 10 mm sapphire NMR tube was purchased from Saphikon, Milford, NH, while the titanium high-pressure charging head was constructed at the ISSECC−CNR (Firenze, Italy).[9] *Note*: *Since high gas pressures are involved, safety precautions must be taken at all stages of studies involving high-pressure NMR tubes.* GC analyses were performed on a Shimadzu GC-14 A gas chromatograph equipped with a flame ionization detector and a 30 m (0.25 mm i.d., 0.25 μm film thickness) SPB-1 Supelco fused silica capillary column. GC/MS analyses were performed on a Shimadzu QP 5000 apparatus equipped with a column identical to that used for GC analyses. The determination of ammonia was performed on a Shimadzu GC-8 A gas chromatograph equipped with a thermal conductivity detector and a 8-ft HayeSep Q 80/100 1/8 in. o.d. stainless steel column (Altech). Infrared spectra were recorded on a Perkin-Elmer 1600 series FT-IR spectrophotometer using samples mulled in Nujol between KBr plates. Elemental analyses (C, H, N) were performed using a Carlo Erba Model 1106 elemental analyzer. Atomic absorption analyses were performed with a Perkin-Elmer 5000 instrument.

2. Catalytic Hydrogenation of BT to DHBT with the Catalyst Precursor 1. A. Parr Reactor Experiments. The reaction conditions and the results of these experiments have been collected in Table 1. In a typical experiment, a solution of **1** (65 mg, 0.043 mmol) and BT (579 mg, 4.3 mmol) in THF (30 mL) was placed into the Parr reactor under nitrogen. After being pressurized with hydrogen to the desired pressure at room temperature, the mixture was heated to the appropriate temperature and then immediately stirred (750 rpm). After the desired time, the reactor was cooled to room temperature and depressurized. The conversion and chemoselectivity of the reaction were determined by GC analysis of the crude reaction mixture. In selected runs, the final solutions were concentrated to dryness in vacuo and the residues, dissolved in THF-d_8, were studied by ^1H and $^{31}P\{^1H\}$ NMR spectroscopy. Several catalytic reactions were carried out in the presence of excess elemental Hg (2000:1) to test the homogeneous character of the reactions. In all cases, no change in both activity and chemoselectivity was observed. Similarly, the catalytic activity did not significantly change when the reactions were carried out in the presence of variable amounts of a colloid-protecting agent such as poly(vinylpyrrolidone) (PVP) (from 0.1% to 100% with respect to the catalyst precursor).

B. Synthesis of DHBT. A solution of **1** (65 mg, 0.043 mmol) and BT (2.885 g, 21.5 mmol) in THF (30 mL) was placed into the Parr reactor under nitrogen. After pressurizing with hydrogen to 30 bar at room temperature, the mixture was heated to 100 °C with stirring (750 rpm). After 1 h, the reactor was cooled to room temperature and depressurized. The contents of the reactor were transferred into a Schlenk-type flask. The solvent was then evaporated under reduced pressure, and the residue, dissolved in *n*-pentane, was passed through a bed of silica (solvent *n*-pentane) to remove the catalyst. The solution was then concentrated to dryness, and DHBT was isolated in quantitative yield. ^1H NMR (CD_2Cl_2, 20 °C): δ 3.30 (m, 4H, H_2-H_3), 6.99 (td, 1H, J(HH) = 7.5, 1.1 Hz, H_6), 7.09 (br t, 1H, J(HP) = 7.3 Hz, H_5), 7.18 (dm, 2H, $H_{4,7}$).

C. Deuteration. A solution of **1** (65 mg, 0.043 mmol) and BT (2.316 g, 17.2 mmol) in THF (30 mL) was placed into the Parr reactor under nitrogen. The system was charged with 15 bar of deuterium and heated to 100 °C with stirring. After 3 h, the reactor was cooled to room temperature and the excess deuterium was vented. The contents of the reactor were transferred into a Schlenk-type flask. GC and GC/MS analysis showed the complete conversion of BT to DHBT-d_2 (*m*/*z* 138) and the formation of NEt_3-d_6 (*m*/*z* 107). The solvent was then evaporated under reduced pressure, and the residue, redissolved in *n*-pentane, was passed through a bed of silica (solvent *n*-pentane) to remove the catalyst. The solution was then concentrated to dryness, and DHBT-d_2 was isolated in quantitative yield. ^1H NMR (CD_2Cl_2, 20 °C): δ 3.24 (dm, 1H, J(HH) = 7.5 Hz, H_3), 3.34 (dm, 1H, J(HH) = 7.5 Hz, H_2), 6.99 (td, 1H, J(HH) = 7.5, 1.1 Hz, H_6), 7.09 (br t, 1H, J(HP) = 7.3 Hz, H_5), 7.18 (dm, 2H, $H_{4,7}$). $^{13}C\{^1H\}$ NMR (CD_2Cl_2, 20 °C): δ 33.6 (1:1:1 t, J(CD) = 21.9 Hz, C_3), 36.5 (1:1:1 t, J(CD) = 20.1 Hz, C_2), 122.7 (s, C_6), 124.8 (s, C_7), 125.2 (s, C_5), 128.0 (s, C_4), 140.9 (s, C), 142.4 (s, C).

When the reaction was carried out at 100 °C for 1 h (64% conversion by GC analysis) or at 30 °C for 5 h (32% conversion), the GC/MS analysis of the reaction mixture showed, besides an identical deuterium enrichment for the product DHBT, no H/D exchange for the remaining BT.

D. Sapphire Tube HPNMR Experiments. A 10 mm sapphire HPNMR tube was charged with a solution of **1** (36 mg, 0.024 mmol) and a 30-fold excess of BT (96 mg, 0.72 mmol) in THF-d_8 (2 mL) under nitrogen. The tube was pressurized with hydrogen to either 30 or 2 bar at room temperature and then placed into a NMR probe at 20 °C. The reaction was followed by variable-temperature $^{31}P\{^1H\}$ and ^1H NMR spectroscopy. The results of this study are detailed in a forthcoming section and illustrated in Figure 2. After the tube was removed from the spectrometer, it was cooled to −40 °C and the gas phase was analyzed by GC. The cool liquid contents of the tube were transferred into a Schlenk-type flask maintained at −40 °C for the GC and GC/MS analysis.

3. Attempted Catalytic Hydrogenations of BT with Other Catalysts. The reactions were performed in the Parr reactor following a procedure analogous to that reported above by substituting $Ru[N(octyl)_4Br]_n$ or $Ru_3(CO)_{12}$ for **1**. A solution of BT (579 mg, 4.3 mmol) in THF (30 mL) was placed into the reactor containing a solid sample of the catalyst (0.043 mmol) under nitrogen. After pressurizing with hydrogen to 30 bar at room temperature, the mixture was heated to 100 °C and then immediately stirred (750−1500 rpm). After the desired time (1−5 h), GC analysis of the crude reaction mixtures gave conversions less than 2%.

4. Reaction of 1 with H_2. A. Parr Reactor Experiment. A solution of **1** (200 mg, 0.13 mmol) in THF (30 mL) was placed into the Parr reactor under a nitrogen atmosphere, pressurized with hydrogen to 30 bar at room temperature, and heated to 60 °C with stirring. After 2 h, the reactor was cooled to room temperature and its contents were evaporated to dryness under vacuum. Analysis by ^1H and $^{31}P\{^1H\}$ NMR spectroscopy of the solid residue showed $[(triphos)Ru(H)(NH_3)_2]BPh_4$ (**5**) and $[(triphos)Ru(H)(NH_3)(NH_2Et)]BPh_4$ (**6**) being present in a 5:1 ratio (see below).

(9) Bianchini, C.; Meli, A.; Traversi, A. CNR; It. Patent FI A000025, 1997.

B. Sapphire Tube HPNMR Experiment. A 10 mm sapphire HPNMR tube was charged with a solution of **1** (36 mg, 0.024 mmol) in THF-d_8 (2 mL) under nitrogen. The tube was pressurized with hydrogen to 30 bar at room temperature and then placed into a NMR probe at 20 °C. The reaction was followed by variable-temperature $^{31}P\{^1H\}$ and ^1H NMR spectroscopy. Partial transformation of **1** occurred already at room temperature yielding **2** and, in minor amount, [(triphos)-Ru(NCMe)$_2$(NH$_3$)](BPh$_4$)$_2$ (**3**, see below). Increasing the temperature to 40 °C led to an increase in the concentration of **2**. At 60 °C, the formation of [(triphos)Ru(H)(NH$_3$)$_2$]BPh$_4$ (**5**) and [(triphos)Ru(H)-(NH$_3$)(NH$_2$Et)]BPh$_4$ (**6**) began to occur. The reaction was complete in ~2 h to give **5** and **6** in a ratio of 5:1. ^1H NMR spectra acquired during all of the experiment showed increasing production of NH$_2$Et, NHEt$_2$, and NEt$_3$. The tube was then removed from the spectrometer and cooled to −40 °C, and the gas phase was analyzed by GC showing the presence of NH$_3$. GC and GC/MS analysis of the solution, maintained at −40 °C, showed the predominant formation of NEt$_3$; NH$_2$Et and NHEt$_2$ were detected only in trace.

5. [(Triphos)Ru(NCMe)$_2$(NH$_3$)](BPh$_4$)$_2$ (3) from 1 and NH$_3$. NMR Experiment. A 5 mm NMR tube was charged first with solid **1** (15 mg, 0.01 mmol) and then with a saturated solution of NH$_3$ in MeCN-d_3 or THF-d_8 (1 mL). The reaction was monitored by $^{31}P\{^1H\}$ and ^1H NMR spectroscopy at room temperature. The ^{31}P NMR singlet of **1** rapidly disappeared; formed in its place were two AM$_2$ spin systems in ~4:1 ratio attributed to **3** and [(triphos)Ru(NCMe)(NH$_3$)$_2$](BPh$_4$)$_2$ (**8**), respectively. Compound **3** is unstable and transformed into **8**, giving, after 2 h, a **3**/**8** ratio of 1:4. $^{31}P\{^1H\}$ NMR: (**3**) δ 32.1 (d, $J(P_MP_A) = 40.8$ Hz, P_M), 24.8 (t, P_A); (**8**) δ 36.1 (t, P_A), 27.8 (d, $J(P_MP_A) = 39.4$ Hz, P_M).

6. [(Triphos)Ru(H)(NCMe)(η^1-*S*-DHBT)]BPh$_4$ (4) from 2 and DHBT. NMR Experiment. An 11 mg (0.01 mmol) amount of **2** was dissolved in a solution of a 20-fold excess of DHBT (25 μL, 0.2 mmol) in THF-d_8 (1 mL). The $^{31}P\{^1H\}$ and ^1H NMR spectra taken immediately after dissolution showed the complete conversion of **2** into **4**. With time, **4** rapidly decomposed, yielding several unidentified species. $^{31}P\{^1H\}$ NMR: AMQ spin system, δ 43.6 (dd, $J(P_AP_M) = 46.6$ Hz, $J(P_AP_Q) = 23.4$ Hz, P_A), 41.6 (dd, $J(P_MP_Q) = 19.2$ Hz, P_M), 10.1 (t, P_Q); ^1H NMR: δ −5.90 (dt, 1H, $J(HP_Q) = 93.6$ Hz, $J(HP_A,P_M) = 19.2$ Hz, Ru-*H*).

7. Synthesis of [(Triphos)Ru(H)(NH$_3$)$_2$]BPh$_4$ (5). Gaseous NH$_3$ was bubbled through a THF (20 mL) solution of **2** (220 mg, 0.2 mmol) at room temperature. After 10 min, the solvent was evaporated under vacuum to ~3 mL. Portionwise addition of *n*-heptane (30 mL) led to the precipitation of **5** as an off-white solid, which was filtered off and washed with *n*-pentane; yield 85%. Anal. calcd (found) for $C_{65}H_{66}BN_2P_3Ru$: C, 72.28 (72.00); H, 6.16 (6.08); N, 2.59 (2.39). $^{31}P\{^1H\}$ NMR (THF-d_8, 20 °C): AM$_2$ spin system, δ 52.8 (d, $J(P_MP_A) = 19.1$ Hz, P_M), 10.5 (t, P_A). ^1H NMR (THF-d_8, 20 °C): δ 2.8−2.2 (m, 6H, CH_2P), 1.85 (s, 6H, NH_3), 1.75 (br q, 3H, CH_3), −5.16 (dt, 1H, $J(HP_A) = 114.4$ Hz, $J(HP_M) = 19.5$ Hz, Ru-*H*). IR: ν(Ru−H) 1830 (s) cm^{-1}.

When the reaction was carried out in an NMR tube (**2** (11 mg, 0.01 mmol) dissolved in a saturated THF-d_8 (1 mL) solution of NH$_3$) and followed by $^{31}P\{^1H\}$ and ^1H NMR spectroscopy, no intermediate species was observed during the conversion of **2** into **5**. When a 5:1 mixture of **5** and **6**, obtained as reported above by hydrogenation of **1**, was employed instead of **2**, only **5** was observed in solution at the end of the reaction.

8. [(Triphos)Ru(H)(NH$_3$)(NH$_2$Et)]BPh$_4$ (6) from 5 and NH$_2$Et. NMR Experiment. A 5 mm NMR tube was charged first with solid **5** (11 mg, 0.01 mmol) and then with a saturated solution of NH$_2$Et in THF-d_8 (1 mL). $^{31}P\{^1H\}$ and ^1H NMR spectroscopy indicated that **6** and [(triphos)Ru(H)(NH$_2$Et)$_2$]BPh$_4$ (**9**) had formed in ~1.5:1 ratio. This ratio remained constant during the following 2 h. $^{31}P\{^1H\}$ NMR: (**6**) AMQ spin system, δ 54.9 (dd, $J(P_AP_M) = 46.7$ Hz, $J(P_AP_Q) = 17.3$ Hz, P_A), 49.9 (dd, $J(P_MP_Q) = 19.4$ Hz, P_M), 9.1 (dt, P_Q); (**9**) AM$_2$ spin system, δ 52.1 (d, $J(P_MP_A) = 19.2$ Hz, P_M), 7.9 (t, P_A). ^1H NMR: (**6**) δ −5.34 (dt, 1H, $J(HP_Q) = 111.8$ Hz, $J(HP_A,P_M) = 20.3$ Hz, Ru-*H*); (**9**) δ −5.49 (dt, 1H, $J(HP_A) = 110.0$ Hz, $J(HP_M) = 21.2$ Hz, Ru-*H*).

9. [(Triphos)Ru(H)(NH$_3$)(η^1-*S*-DHBT)]BPh$_4$ (7) from 5 and DHBT. NMR Experiment. An 11 mg (0.01 mmol) amount of **5** was dissolved in a THF-d_8 (1 mL) solution of a 20-fold excess of DHBT (25 μL, 0.2 mmol). The $^{31}P\{^1H\}$ and ^1H NMR spectra taken immediately after dissolution showed the complete conversion of **5** into **7**. Compound **7** is unstable and decomposed completely within 2 h, yielding several unidentified species. $^{31}P\{^1H\}$ NMR: AMQ spin system, δ 46.8 (dd, $J(P_AP_M) = 46.7$ Hz, $J(P_AP_Q) = 18.5$ Hz, P_A), 42.8 (dd, $J(P_MP_Q) = 23.3$ Hz, P_M), 13.0 (dd, P_Q). ^1H NMR: δ −5.73 (dt, 1H, $J(HP_Q) = 94.1$ Hz, $J(HP_A,P_M) = 19.1$ Hz, Ru-*H*).

10. HPNMR Reaction of 1 with H$_2$ and BT in THF-d_8/H$_2$O. A 10 mm sapphire tube was charged with a THF-d_8/H$_2$O (19:1, v/v, 2 mL) solution of **1** (36 mg, 0.024 mmol) and a 30-fold excess of BT (96 mg, 0.72 mmol) under nitrogen. The tube was pressurized with hydrogen to 30 bar at room temperature and then placed into a NMR probe at 20 °C. The reaction was followed by variable-temperature $^{31}P\{^1H\}$ and ^1H NMR spectroscopy. Partial transformation of **1** occurred at room temperature, yielding a new noncontaining hydride compound (**10**), characterized by a $^{31}P\{^1H\}$ NMR AM$_2$ pattern (δ 40.4 (t, P_A), 26.2 (d, $J(P_MP_A) = 38.7$ Hz, P_M)), and **2**, as minor species. Increasing the temperature to 60 °C led to the quantitative conversion of **1** and all the previously formed compounds to [(triphos)Ru(O$_2$CCH$_3$)(OH$_2$)]BPh$_4$ (**11**, see below) and the known dimer [(triphos)Ru(μ-OH)$_3$Ru(triphos)]-BPh$_4$[7] (**12**) in a ~4:2 ratio based on the (triphos)Ru moiety. In the following 2 h at 60 °C, no new ruthenium species formed and the **11** to **12** ratio remained constant. The ^1H NMR spectra, acquired over all the experiment at 60 °C, showed the formation of DHBT only in the first spectrum; no appreciable increase of its concentration was observed in the following 2 h. After the NMR probe was cooled to room temperature, **11** and **12** were still the only metal products visible by $^{31}P\{^1H\}$ NMR spectroscopy. GC analysis of the solution confirmed the scarce production of DHBT (15%). All of our attempts to unambiguously identify **10** were unsuccessful due to its low concentration at any stage of the reaction. Since **10** was also observed at the early stages of the reaction between **1** in THF and water to give the dimer **12**, its probable formulation is [(triphos)Ru(NCMe)$_2$(H$_2$O)]$^{2+}$.

11. HPNMR Reaction of 1 with H$_2$ in THF-d_8/H$_2$O, Followed by Treatment with BT and H$_2$. A 10 mm sapphire tube was charged with a THF-d_8/H$_2$O (19:1, v/v, 2 mL) solution of **1** (36 mg, 0.024 mmol). The tube was pressurized with hydrogen to 30 bar at room temperature and then placed into a NMR probe at 20 °C. The reaction was followed by variable-temperature $^{31}P\{^1H\}$ and ^1H NMR spectroscopy. As in the above experiment, partial transformation of **1** occurred at room temperature, yielding **10** and **2**. Increasing the temperature to 60 °C led to the formation of **11** and **12** in a ~4:2 ratio. After 1 h, the NMR probe was cooled to room temperature and the tube was charged with a 30-fold excess of BT (96 mg, 0.72 mmol) and 30 bar of hydrogen. The tube was placed into a NMR probe and heated at 60 °C for 2 h. During all of this period, compounds **11** and **12** were the only metal products visible by $^{31}P\{^1H\}$ NMR spectroscopy and no production of DHBT was observed by ^1H NMR spectroscopy. GC analysis of the final solution confirmed the lack of conversion of BT to DHBT.

12. [(Triphos)Ru(O$_2$CCH$_3$)(OH$_2$)]BPh$_4$ (11) from 1 and CH$_3$-COOH. NMR Experiment. Neat CH$_3$COOH (2 μL, 0.03 mmol) was syringed into a 5 mm NMR tube containing a solution of **1** (15 mg, 0.01 mmol) in THF-d_8/H$_2$O (19:1, v/v, 2 mL). The $^{31}P\{^1H\}$ and ^1H NMR spectra taken immediately after the addition showed the complete conversion of **1** into **11**. $^{31}P\{^1H\}$ NMR: AM$_2$ spin system, δ 46.0 (d, $J(P_MP_A) = 40.8$ Hz, P_M), 29.3 (t, P_A). ^1H NMR: δ 2.21 (s, 3H, CH_3-CO$_2$).

13. Kinetic Measurements. In a typical experiment, a solution of the catalyst and the substrate in tetrahydrofuran was placed in a glass reactor fitted with a reflux condenser kept at 0 °C. The reactor was sealed with Apiezon wax to a high-vacuum line, and the solution was carefully degassed by three freeze−pump−thaw cycles; hydrogen was admitted at this point to the desired pressure, an electric oven preheated to the required temperature was placed around the reactor, and magnetic stirring was immediately commenced. The reaction was followed by measuring the hydrogen pressure drop as a function of time.[10] Each run was repeated at least twice to ensure reproducibility of the results.

The conversion of reactants in the catalytic reactions was generally (although not necessarily) kept below 10% in order to use the initial

(10) Sánchez-Delgado, R. A.; Andriollo, A.; Puga, J.; Martín, G. *Inorg. Chem.* **1987**, *26*, 1867.

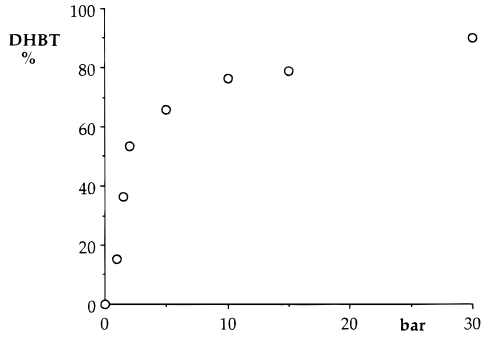

Figure 1. Dependence of the DHBT production on the hydrogen pressure for reactions at 40 °C (see Table 1, runs 5−11).

rates method in our calculations. The measured $\Delta P(H_2)$ values were converted to millimoles of DHBT produced, and the data were plotted as molar concentration of the product as a function of time, yielding straight lines. Initial rates were then obtained from the corresponding slopes. All of the straight lines were fitted by use of conventional linear regression software to $r^2 > 0.98$. Concentrations of dissolved hydrogen were calculated using published solubility data.[11]

Results

Autoclave Reactions. The regioselective hydrogenation of BT to DHBT in THF is efficiently catalyzed by [(triphos)Ru(NCMe)$_3$](BPh$_4$)$_2$ (**1**) under mild conditions (Table 1).

At 100 °C and 30 bar of H_2 (entry 1), BT is converted to DHBT with an average rate of 500 (expressed as mol of product (mol of catalyst)$^{-1}$ h^{-1}), which is the highest homogeneous value ever reported.[6,12] The catalytic activity is quite acceptable also at 60 and 40 °C with rates of 93 and 46, respectively (entries 3 and 4). For a substrate-to-catalyst ratio of 100 and 40 °C, all BT is hydrogenated in ∼5 h at 30 bar of H_2 (entry 5). Decreasing the pressure decreases the hydrogenation rate (entries 6−11). As one may readily infer by plotting the conversion vs the H_2 pressure (Figure 1), a change of the reaction kinetics apparently occurs on going from low to high pressure, however. In particular, from 1 to 2 bar, the rate increases proportionally with the pressure (entries 9−11); above 5 bar the rate almost levels off.

Several experiments were carried out substituting D_2 for H_2. In all cases, the selective *cis*-deuteration[12c] of BT to DHBT-d_2 (parent ion at *m*/*z* 138) occurred as evidenced by the ^{1}H NMR spectra, showing two doublets of multiplets at δ 3.24 (H_3) and 3.34 (H_2) with J(HH) = 7.5 Hz (eq 2). Deuterium enrichment was observed in neither the unreacted BT nor the arene ring of DHBT.

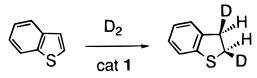

(2)

The homogeneity of the hydrogenation runs was inferred from the high selectivity observed, together with an excellent reproducibility of the kinetic measurements (vide infra), and from the fact that the addition of elemental mercury to the solutions did not affect the catalytic rates.[13] In particular, the formation of a highly dispersed colloidal ruthenium catalyst was ruled out by experiments carried out in the presence of either variable amounts of PVP, which showed no change of activity,[14] or Ru[N(octyl)$_4$Br]$_n$, which showed negligible conversion to DHBT. Similarly, the substitution of $Ru_3(CO)_{12}$ for **1** did not afford a catalytic reaction.

At the end of the catalytic reactions with **1**, all of the ruthenium was recovered in the form of monohydrido complexes of the formula [(triphos)Ru(H)(L)(L′)]BPh$_4$, where L and L′ may be NH_3, $NHEt_2$, MeCN, or η^1-*S*-DHBT, depending on the H_2 pressure. In particular, below 5 bar of H_2, the nitrile was not reduced even at 100 °C. Accordingly, for the reactions carried out at 30 bar and ≥60 °C, the termination metal products were [(triphos)Ru(H)(NH$_3$)$_2$]BPh$_4$ (**5**), [(triphos)Ru(H)(NH$_3$)(NH$_2$-Et)]BPh$_4$ (**6**), and [(triphos)Ru(H)(NH$_3$)(η^1-*S*-DHBT)]BPh$_4$ (**7**), while the reactions at 40 °C and 1−2 bar yielded exclusively [(triphos)Ru(H)(NCMe)(η^1-*S*-DHBT)]BPh$_4$ (**4**). All of these Ru(II) monohydrido complexes as well as others formed during the catalytic reactions were identified by comparison of their ^{31}P{^{1}H} and ^{1}H NMR spectra with those of authentic specimen independently synthesized (see below).

As already reported by us,[7] the formation of the amine complexes is a consequence of the Ru-assisted hydrogenation of the MeCN ligands in **1** to the primary amine NH_2Et, followed by an amine redistribution reaction which generates $NHEt_2$, NEt_3, and NH_3.[15] Indeed, all of these amine byproducts have been found to form in both autoclave and in situ reactions and have been authenticated by ^{1}H NMR or GC/MS analysis.

The formation of the hydride ligand in all complexes apparently occurs via heterolytic splitting of H_2[12e,16] and does not necessarily involve the assistance of the amine products as complex **4** is generated also in experimental conditions (40 °C, 2 bar H_2) at which the nitrile is not reduced at all.

Notably, all the monohydrido Ru(II) complexes previously described catalyze the regioselective hydrogenation of BT to DHBT as efficiently as the catalyst precursor **1**. The present catalyst system for the hydrogenation of BT is thus exceptionally robust and can easily and quantitatively be recycled on the condition that the solvent is reasonably anhydrous. Indeed, the catalytic activity is so high that 500 equiv of BT was hydrogenated to DHBT with **1** in 1 h even when 1.5 mL of water was added to the initial THF solution of **1** (entry 2); the termination Ru products recovered after catalysis, however, showed a marked decrease in the catalytic activity (∼75%). An independent HPNMR study has revealed that, in catalytic conditions, water in the reaction mixture slowly converts the precursor **1** to a mixture of the acetate-aquo complex [(triphos)Ru(O$_2$CCH$_3$)(OH$_2$)]BPh$_4$ (**11**) and of the known dimer [(tri-

(11) Young, C. L., Ed.; Solubility Data Series IUPAC; Pergamon: Oxford, U.K., 1981; Vol. 516, p 219.

(12) (a) Herrera, V.; Fuentes, A.; Rosales, M.; Sánchez-Delgado, R. A.; Bianchini, C.; Meli, A.; Vizza, F. *Organometallics* **1997**, *16*, 2465. (b) Sánchez-Delgado, R. A.; Herrera, V.; Rincón, L.; Andriollo, A.; Martín, G. *Organometallics* **1994**, *13*, 553. (c) Baralt, E.; Smith, S. J.; Hurwitz, J.; Horváth, I. T.; Fish, R. H. *J. Am. Chem. Soc.* **1992**, *114*, 5187. (d) Fish, R. H.; Tan, J. L.; Thormodsen, A. D. *J. Org. Chem.* **1984**, *49*, 4500. (e) Bianchini, C.; Meli, A.; Patinec, V.; Sernau, V.; Vizza, F. *J. Am. Chem. Soc.* **1997**, *119*, 4945. (f) Bianchini, C.; Herrera, V.; Jiménez, M. V.; Meli, A.; Sánchez-Delgado, R. A.; Vizza, F. *J. Am. Chem. Soc.* **1995**, *117*, 8567.

(13) Lin, Y.; Finke, R. G. *Inorg. Chem.* **1994**, *33*, 4891.

(14) (a) Wang, Q.; Liu, H.; Han, M.; Li, X.; Jiang, D. *J. Mol. Catal., A* **1997**, *118*, 145. (b) Hirai, H.; Chawanya, H.; Toshima, H. *Bull. Chem. Soc. Jpn.* **1985**, *58*, 682.

(15) (a) Joshi, A. M.; MacFarlane, K. S.; James, B. R.; Frediani, P. *Chem. Ind.* **1994**, *53*, 497. (b) Jung, C. W.; Fellmann, J. D.; Garrou, P. E. *Organometallics* **1983**, *2*, 1042. (c) Holy, N. L. *J. Org. Chem.* **1979**, *44*, 239.

(16) (a) Sellmann, D.; Rackelmann, G. H.; Heinemann, F. W. *Chem. Eur. J.* **1997**, *3*, 2071. (b) Bianchini, C.; Casares, J. A.; Meli, A.; Sernau, V.; Vizza, F.; Sánchez-Delgado, R. A. *Polyhedron* **1997**, *16*, 3099. (c) Bianchini, C.; Fabbri, D.; Gladiali, S.; Meli, A.; Pohl, W.; Vizza, F. *Organometallics* **1996**, *15*, 4604. (d) Buriak, J. M.; Osborn, J. A. *Organometallics* **1996**, *15*, 3161. (e) Sierraalta, A.; Ruette, F. *J. Mol. Catal., A* **1997**, *109*, 227. (f) Szalontai, B.; Joó, F.; Papp, E.; Vígh, L. *J. Chem. Soc., Chem. Commun.* **1995**, 2299. (g) Topsøe, N.; Topsøe, H. *J. Catal.* **1993**, *139*, 641. (h) Jessop, P. G.; Morris, R. H. *Coord. Chem. Rev.* **1992**, *121*, 155. (i) Lang, J. F.; Masel, R. I. *Surf. Sci.* **1987**, *183*, 44. (j) Bianchini, C.; Mealli, C.; Meli, A.; Sabat, M. *Inorg. Chem.* **1986**, *25*, 4617.

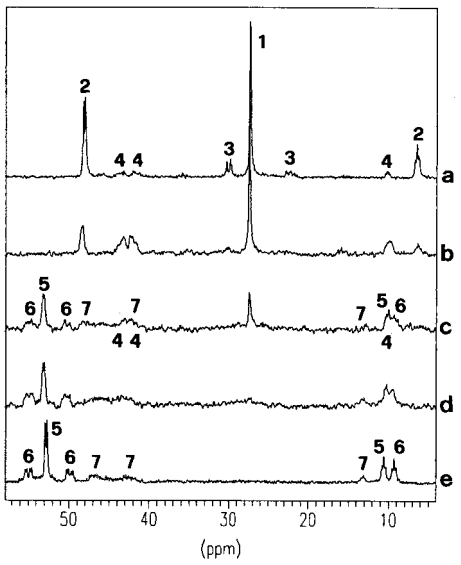

Figure 2. $^{31}P\{^1H\}$ NMR study (sapphire tube, THF-d_8, 81.01 MHz) of the catalytic hydrogenation of BT in the presence of **1** (30 bar H_2, substrate/catalyst ratio 30): (a) at 20 °C for 30 min; (b) at 60 °C; (c) at 60 °C for 60 min; (d) at 60 °C for 90 min; (e) after the tube was cooled to room temperature.

phos)Ru(μ-OH)$_3$Ru(triphos)]BPh_4 (**12**),[7] which are inactive for the hydrogenation of BT. While the formation of μ-hydroxo dimers has precedents in the literature for phosphine−ruthenium complexes in aqueous media,[17] the obtainment of the acetate complex **11** is quite surprising in the absence of oxygen and alcohols.[18] We think that the acetate ligand is formed by hydration of MeCN, a reaction which is typically catalyzed by either protic acids[19a] (in the actual catalytic mixture, protons can be generated upon formation of **12** or by heterolytic splitting of H_2) or hydrido Ru complexes via amide intermediates.[19b]

HPNMR Studies. A sequence of selected $^{31}P\{^1H\}$ NMR spectra in TFH-d_8 for the hydrogenation of BT catalyzed by **1** at 30 bar of H_2 is reported in Figure 2.

Upon reaction of **1** with H_2, partial transformation of **1** occurred at room temperature, yielding the known Ru(II) hydrido complex [(triphos)Ru(H)(NCMe)$_2$]BPh_4[7] (**2**) as the predominant product together with minor amounts of the ammonia complex [(triphos)Ru(NCMe)$_2$(NH$_3$)](BPh$_4$)$_2$ (**3**) and of the DHBT adduct **4** (trace a). Increasing the temperature to 60 °C led to an increase in the concentration of **4** (trace b). With time, **1** and all of the previously formed species converted to **5**, **6**, and **7** (traces c and d, after 60 and 90 min, respectively). After the NMR probe was cooled to room temperature, **5**, **6**, and **7** (ratios 5:5:1) were still the only metal products visible by $^{31}P\{^1H\}$ NMR spectroscopy (trace e). ^1H NMR spectra acquired during the experiment showed a gradual increase in the concentration of DHBT at the expense of that of BT and the formation of NH_2Et, $NHEt_2$, and NEt_3. The tube was then removed from the spectrometer and cooled to −40 °C, and the gas phase was analyzed by GC showing the presence of NH_3. The cool liquid contents of the tube were then transferred into a Schlenk-type flask maintained at −40 °C. GC and GC/MS analysis of the solution showed the conversion of BT to DHBT (87%) and the formation of NEt_3 and $NHEt_2$ in a ratio of 3:1; NH_2Et was detected only in trace amount.

The hydrogenation of BT to DHBT was studied by NMR spectroscopy also at low H_2 pressure (2 bar). At this pressure, a little compound **1** converted exclusively to **2**. Increasing the temperature to 60 °C led to a modest increase in the concentration of **2** and to the formation of a small amount of **4**. With time, most of **1** remained unreacted and only **2** and **4** were visible by $^{31}P\{^1H\}$ NMR spectroscopy. No formation of **5**, **6**, or **7** was observed. After the NMR probe was cooled to room temperature, **1**, **2**, and **4** were still the only metal products visible by $^{31}P\{^1H\}$ NMR spectroscopy. ^1H NMR spectra acquired during the experiment showed a slow increase in the concentration of DHBT at the expense of that of BT and no formation of NH_2Et, $NHEt_2$, and NEt_3, while a GC analysis of the gas phase in the headspace of the tube showed the absence of NH_3. The conversion of BT to DHBT was 38%.

Consistent with the above NMR experiment, catalytic reactions in autoclaves with 2 bar of H_2 gave satisfactory conversions to DHBT, but no production of amines was observed, while all of the ruthenium metal was recovered as the DHBT adduct **4**.

Synthesis and Characterization of the Ruthenium Complexes Detected During the Catalytic Reactions. With the use of isolated compounds in independent reactions, almost all compounds seen during the in situ HPNMR experiments or isolated at the end of the batch reactions have unambiguously been identified. Scheme 2 illustrates the reactions performed and the products obtained. These have been listed following a sequence which is as close as possible to that seen by in situ NMR spectroscopy in the catalytic reactions.

Most of the transfomations described in Scheme 2 are typical ligand-substitution reactions that occur quite rapidly in THF at room temperature using an excess of the substituting ligand (a, b, d, e). Only reaction c represents a multistep and complex chemical transformation as it comprises a heterolytic splitting of H_2 to give the terminal hydride,[12e,16] the reduction of MeCN to NH_2Et (most likely via imine intermediate), and the conversion of the primary amine to secondary and tertiary amines with concomitant extrusion of NH_3. The overall transformation pattern undergone by the MeCN ligands in **1** is well-known for homogeneous Ru(II) catalysts.[7,15]

The characterization of the complexes shown in Scheme 2 is quite straightforward and does not need any specific comment. When the complexes bear two identical ligands, the $^{31}P\{^1H\}$ NMR spectra consist of first-order AM_2 patterns while AMQ patterns are exhibited by the complexes with three different ligands trans to the phosphorus atoms. The resonance of the terminal hydride ligands appears as a doublet of triplets also for the ^{31}P AMQ patterns due to the fortuitous coincidence of the J(HP) values. Among the complexes shown in Scheme 2, only **2**, **5**, and **6** were isolated in the solid state; all of the other compounds were prepared and characterized exclusively in solution due to their inherent instability in the solid state.

Kinetic Studies. The kinetics of the hydrogenation of BT to DHBT were studied by measuring the hydrogen pressure drop in THF; runs were performed at different catalyst, substrate, and hydrogen concentrations and at different temperatures. Conversions were kept below 10% in order to apply an initial rate treatment in our kinetic analysis. The complete data are listed in Table 2.

(17) (a) Burn, M. J.; Fickes, M. G.; Hartwig, J. F.; Hollander, F. J.; Bergman, R. G. *J. Am. Chem. Soc.* **1993**, *115*, 5875. (b) Frediani, P.; Bianchi, M.; Piacenti, F.; Ianelli, S.; Nardelli, M. *Inorg. Chem.* **1987**, *26*, 1592. (c) Ashworth, T. V.; Nolte, M. J.; Singleton, E. *J. Chem. Soc., Chem. Commun.* **1971**, 936.

(18) (a) Bianchini, Meli, A.; Peruzzini, M.; Vizza, F. *J. Am. Chem. Soc.* **1990**, *112*, 6726. (b) Christian, D. F.; Clark, G. R.; Roper, W. R.; Waters, J. M.; Whittle, K. R. *J. Chem. Soc., Chem. Commun.* **1972**, 458.

(19) (a) March, J. *Advanced Organic Chemistry*, 4th ed.; Wiley-Interscience: New York; pp 887−888. (b) Murahashi, S.-I.; Sasao, S.; Saito, E.; Naota, T. *Tetrahedron* **1993**, *49*, 8805.

Scheme 2

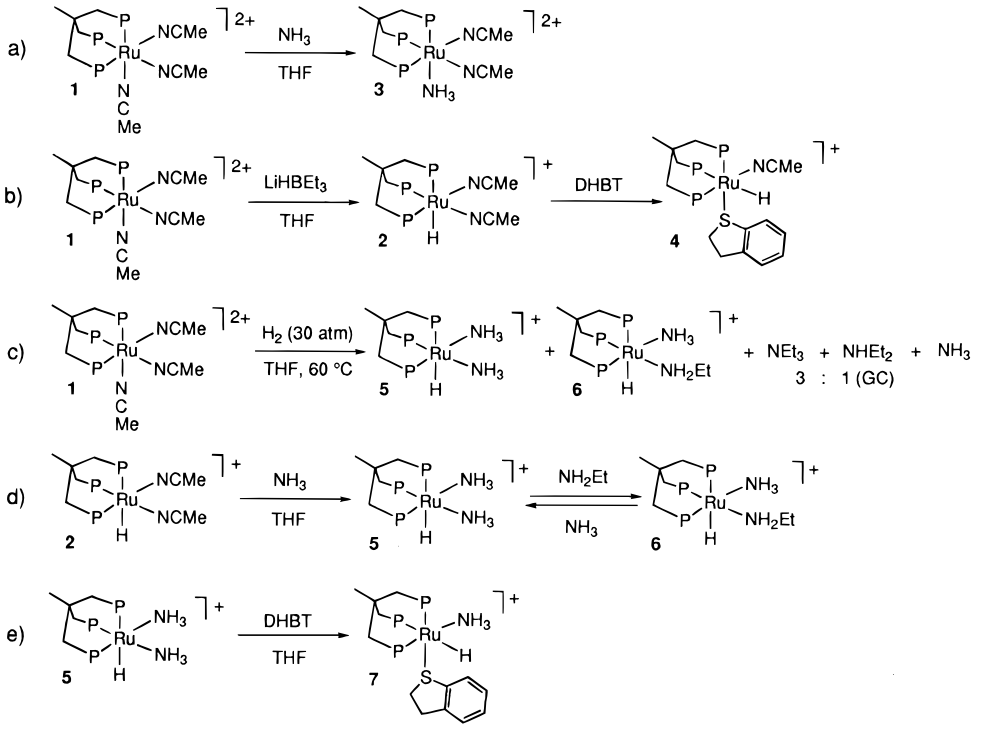

Table 2. Kinetic Data for the Hydrogenation of Benzothiophene with $[(Triphos)Ru(NCMe)_3](BPh_4)_2$ (**1**) as the Catalyst Precursor[a]

T (K)	10^4 [Ru] (M)	10^2 [BT] (M)	10^5 [H_2] (M)	10^6 r_i (M s^{-1})	conversion (%)	turnover
319	4.0	5.0	6.0	1.08	9.9	12.4
319	6.0	5.0	6.0	1.81	10.2	8.5
319	8.0	5.0	6.0	2.23	8.3	5.2
319	10.0	5.0	6.0	2.62	7.5	3.8
319	6.0	2.5	6.0	1.01	6.8	5.7
319	6.0	7.4	6.0	2.31	6.6	8.1
319	6.0	10.0	6.0	3.09	7.7	12.8
319	6.0	5.0	4.3	1.32	5.7	4.8
319	6.0	5.0	5.1	1.52	5.9	4.9
319	6.0	5.0	6.8	2.06	6.3	5.3
299	6.0	5.0	6.0	0.36	6.4	5.3
309	6.0	5.0	6.0	0.90	8.0	6.7
333	6.0	5.0	6.0	3.53	7.8	6.5

[a] Solvent: tetrahydrofuran (50 mL); r_i = initial rates.

The initial rates of hydrogenation of BT (r_i) were found to be first-order with respect to catalyst and hydrogen concentrations and close to first-order with respect to substrate concentration (as determined by plots of log r_i vs log [Ru], log r_i vs log [H_2], and log r_i vs log [BT], which yielded straight lines of slope 1.0, 1.0, and 0.8, respectively; see Figures 3−5, Supporting Information).

Consequently, the experimental rate law can be written as the following:

$$d[DHBT]/dt = k_{cat}[Ru][BT][H_2] \quad (3)$$

The value for the catalytic rate constant at 319 K was calculated from eq 3: $k_{cat} = 1.01 \times 10^3$ M^{-2} s^{-1}.

The effect of the temperature on the rate constant was studied in the range 299−333 K for concentrations of BT at 5.0×10^{-2} M, catalyst at 6.0×10^{-4} M, and dissolved hydrogen at 6.0×10^{-5} M. Within the range of conditions used, the variation of the solubility of hydrogen with the temperature is negligible.[11] A plot of ln k_{cat} vs $1/T$ (Figure 6, Supporting Information) allowed us to evaluate the activation energy E_a, the frequency factor A, the extrapolated value of the rate constant at 298 K, and the values of enthalpy, entropy, and free energy of activation (calculated from the equations $\Delta H^{\ddagger} = E_a - RT$; $\Delta S^{\ddagger} = R$ ln(hA/e^2k_BT), and $\Delta G^{\ddagger} = \Delta H^{\ddagger} - T\Delta S^{\ddagger}$, respectively); these values are listed in Table 3.

Table 3. Activation Parameters for the Hydrogenation of Benzothiophene with $[(Triphos)Ru(NCMe)_3](BPh_4)_2$ (**1**) as the Catalyst Precursor

E_a (kcal/mol)	13.3 ± 0.5
A (M^{-1} s^{-1})	$(2.1 \pm 0.5) \times 10^{12}$
k_{cat} (25 °C) (M^{-2} s^{-1})	2.06×10^2
$\Delta H^{\ddagger}$ (kcal/mol)	12.7 ± 0.6
$\Delta S^{\ddagger}$ (eu)	-9.2 ± 0.8
$\Delta G^{\ddagger}$ (kcal/mol)	16 ± 3

Discussion

The Mechanism of the Hydrogenation of Benzo[*b*]-thiophene. The reactor and HPNMR studies described above show that complex **1** reacts readily with H_2 to yield $[(triphos)-RuH(L)_2]^+$, which is the species actually entering the catalytic cycle. Under 30 bar H_2 the coordinated acetonitrile was found by HPNMR and GC-MS to be transformed into a mixture of NH_2Et, $NHEt_2$, NEt_3, and NH_3, which may be free in solution or coordinated to Ru, and thus L can be the nitrile or the amines under high pressure. These amines, present in very small quantities, are considered very labile and do not seem to intervene in the overall reaction. At the low pressures used in the kinetic study, acetonitrile was not hydrogenated to any appreciable extent, and therefore under those conditions L is MeCN or the solvent THF. For the sake of clarity, the labile L ligands will be omitted in the discussion to follow and in the catalytic cycle proposed below.

The observed low pressure kinetics can be interpreted in terms of the following set of equations: BT coordinates readily and reversibly to $[(triphos)RuH]^+$ (**A**) to form $[(triphos)RuH(BT)]^+$ (**B**) (eq 4):

$$\underset{\mathbf{A}}{[(\text{triphos})\text{RuH}]^+} + \text{BT} \overset{K_1}{\rightleftharpoons} \underset{\mathbf{B}}{[(\text{triphos})\text{RuH(BT)}]^+} \quad (4)$$

An irreversible (deuterium labeling experiments) reaction of **B** with H_2 takes place to yield $[(\text{triphos})\text{Ru(DHBT)}]^+$ (**C**) as shown in eq 5:

$$\underset{\mathbf{B}}{[(\text{triphos})\text{RuH(BT)}]^+} + \text{H}_2 \xrightarrow{k_2} \underset{\mathbf{C}}{[(\text{triphos})\text{RuH(DHBT)}]^+} \quad (5)$$

The subsequent reversible dissociation of the product DHBT from **C** (eq 6) regenerates the active hydride and completes the catalytic cycle:

$$\underset{\mathbf{C}}{[(\text{triphos})\text{RuH(DHBT)}]^+} \overset{K_3}{\rightleftharpoons} \underset{\mathbf{A}}{[(\text{triphos})\text{RuH}]^+} + \text{DHBT} \quad (6)$$

According to this mechanism, a rate law can be derived, taking into account that the rate of hydrogen consumption is the following:

$$-\text{d}[\text{H}_2]/\text{d}t = k_2[\mathbf{B}][\text{H}_2] \quad (7)$$

Considering the equilibria shown in eqs 4 and 6 and the mass balance for ruthenium ($[\text{Ru}]_0 = [\mathbf{A}] + [\mathbf{B}] + [\mathbf{C}]$) and substituting [**B**] in eq 7, the rate expression becomes the following:

$$-\text{d}[\text{H}_2]/\text{d}t = \frac{K_1k_2K_3}{K_3 + K_1K_3[\text{BT}] + [\text{DHBT}]}\,[\text{Ru}]_0[\text{BT}][\text{H}_2] \quad (8)$$

Since at low pressure we measured only *initial* rates (r_i, BT conversions below 10%), the concentration of DHBT in solution under those conditions is very small and the term [DHBT] can be ignored in eq 8, the rate law becoming the following:

$$r_i = \frac{K_1k_2}{1 + K_1[\text{BT}]}\,[\text{Ru}]_0[\text{BT}][\text{H}_2] \quad (9)$$

which is identical to our experimentally determined law for

$$k_{cat} = \frac{K_1k_2}{1 + K_1[\text{BT}]} \quad (10)$$

inverting and reorganizing eq 9 leads to the following:

$$\frac{[\text{Ru}]_0[\text{H}_2]}{r_i} = \frac{1}{k_2} + \frac{1}{K_1k_2[\text{BT}]} \quad (11)$$

and therefore a plot of $[\text{Ru}]_0[\text{H}_2]/r_i$ vs 1/[BT] is a straight line (Figure 7, Supporting Information), which allows us to obtain values for k_2 (278.4 M^{-1} s^{-1}) and K_1 (4.5 M^{-1}).

At low substrate concentrations, $K_1[\text{BT}] \ll 1$ and the rate expression can be approximated to

$$r_i = K_1k_2[\text{Ru}]_0[\text{BT}][\text{H}_2] \quad (12)$$

which is also identical to the experimental rate law observed at low pressures if $k_{cat} = K_1k_2$. Within the range of BT concentrations used in this study, $K_1[\text{BT}] = 0.11-0.45$ and thus at the higher substrate concentrations the $K_1[\text{BT}]$ term should not be neglected, which explains the slightly low (0.8) overall rate dependence on [BT].

Scheme 3. Proposed Catalytic Cycle for the Hydrogenation of BT by Complex **1**[a]

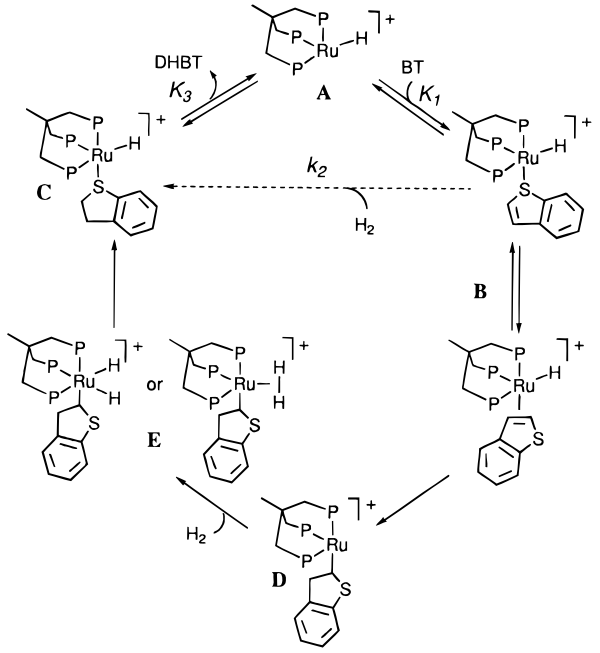

[a] Ligands L = MeCN or THF complete the coordination sphere in all species depicted but have been omitted for clarity.

On the other hand, at the high conversions measured in the autoclave experiments, particularly at pressures higher than 2 bar, the concentrations of BT are low and those of DHBT are high, and consequently the rates tend to level off, as would be predicted from eq 8; this is indeed the behavior observed in Figure 1.

Although the kinetic data alone only allow the interpretation represented by eqs 4−6, involving the intermediates **A**, **B**, and **C**, the accumulated results, together with previous knowledge on BT hydrogenation reactions,[4,6,12] are in agreement with the catalytic cycle represented in Scheme 3, which merits a few additional comments.

The formation of species **A** has been demonstrated by the independent preparative and in situ NMR experiments described above on the reaction of **1** with hydrogen to yield $[(\text{triphos})\text{-RuH(L)}_2]^+$, where L is MeCN or amines depending on the H_2 pressure.

BT is known to coordinate metal fragments yielding η^1-*S* or η^2-*C,C* adducts or equilibria between these two bonding modes.[4] The η^2-BT coordination mode, however, is generally accepted to be the crucial one for the hydrogenation of the thiophenic ring.[4d,g] Hydride migration has previously been proposed to take place onto Cα or Cβ to produce a 3- or 2-benzothienyl complex, respectively.[4d,g] On the basis of theoretical studies including recent ab initio calculations, a 2-benzothienyl intermediate is most likely, indeed.[20] Oxidative addition of H_2 to a Ru(II) species such as **D** is a well-known process, eventually occurring via an η^2-H_2−Ru intermediate.[16h]

Transfer of the second hydride to coordinated HBT generates the complex $[(\text{triphos})\text{RuH(DHBT)}]^+$ (**C**), which was actually observed by in situ NMR measurements as the MeCN adduct **4**. The fact that only **A** and **C** were observed by NMR during the in situ catalytic experiments, together with the fact that no deuterium incorporation was observed in either unreacted BT

(20) Hinchliffe, J. *Mol. Struct.* **1995**, *334*, 235.

or the arene ring of DHBT, indicates that the transfer of hydrides to coordinated BT is rapid and irreversible, while coordination of BT to **A** and dissociation of DHBT to regenerate **A** and restart the cycle must be reversible reactions.

This mechanism differs from the one previously deduced for the hydrogenation of BT by Rh− and Ir−PPh_3 complexes, in that the latter displayed a zero-order dependence on substrate concentration and a rate-limiting hydride transfer to coordinated BT.[12a] Otherwise, the elementary steps which compose the proposed cycle are similar to the ones described in other BT hydrogenation mechanisms and closely related to well-known C═C bond hydrogenation cycles.

Stabilization and Deactivation Pathways of the Ruthenium Catalysts. The presence of catalytic amounts of nitrogen ligands (MeCN, amines) in the hydrogenation reactions assisted by $[(triphos)RuH]^+$ does not apparently inhibit the catalytic activity, though MeCN, NH_3, or $NHEt_2$ is capable of forming adducts that are seen during the reactions and all the termination ruthenium products contain amine ligands. Nitrogen compounds (quinoline, aniline) have recently been found to increase the rate of hydrogenation of BT by water-soluble ruthenium complexes in aqueous biphase reactions.[6a] The nitrogen bases have been claimed to either stabilize the catalytically active species or accelerate its formation from the catalyst precursor. In our reactions, the nitrogen ligands are certainly important for the stabilization and the recycling of the catalytically active species $[(triphos)RuH]^+$ through the formation of stable termination products. Indeed, preliminary results with the catalyst precursor $[(triphos)Ru(DMSO)_2(H_2O)](SO_3CF_3)_2$[21] show that the hydrogenation of BT to DHBT is initially as fast as that with **1** (DMSO = dimethyl sulfoxide).[22] The deactivation of the DMSO-containing catalysts is much faster, however, probably because of the absence of nitrogen ligands in the reaction mixture.

As described in a previous section, the poisoning effect of water toward $[(triphos)RuH]^+$ is not simply due to the formation of strong coordinative adducts, although water is evidently a better ligand than acetonitrile or amines for this fragment. Indeed, the deprotonation of coordinated water seems to be a facile process at Ru(II), and the resulting hydroxy groups, particularly in the μ-bonding mode, form very stable adducts which do not react with either BT or H_2 in the experimental conditions investigated. The poisoning of the present Ru(II) catalysts by oxygen donors, particularly in anionic form, is further on confirmed by the inactivity of the acetate complex **11** for the hydrogenation of BT.

The Activation of Benzo[*b*]thiophene by the Isostructural but not Isoelectronic $[(triphos)RuH]^n$ ($n = +1, -1$) Fragments. In a previous paper, we have reported that the Ru(0) $16e^-$ fragment $[(triphos)RuH]^-$ is a selective catalyst for the hydrogenolysis of BT to ETP in THF at 100 °C and 30 bar of H_2 (eq 13).[7] Under these experimental conditions, the catalyst was inactive for the hydrogenolyis of DHBT.7

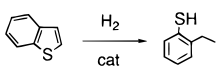

(3)

The mechanism proposed for this hydrogenolysis reaction is illustrated in Scheme 4. Herein we have shown that the two-electron oxidation of the ruthenium center results in a dramatic change of the chemoselectivity of the hydrogenation of BT

Scheme 4

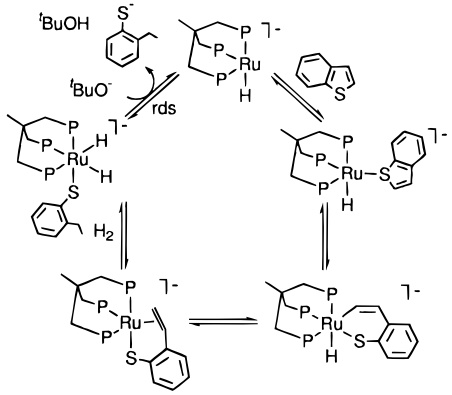

which, in comparable experimental conditions, is exclusively converted to the thioether.

It has amply been demonstrated that BT may approach a coordinatively metal fragment using either the sulfur atom or the proximal C_2-C_3 double bond.[5b,23] In the former case, the cleavage of the C−S bond may eventually take place provided the metal possesses the appropriate electron density for the $d\pi$-(metal) π^*(C−S) transfer[24] (hydrogenolysis path when either H_2 or hydride ligands are involved in the C−S scission step). Otherwise, when BT binds the metal like an olefin, the hydrogenation of the double bond may occur via hydride transfer (hydrogenation path) (Scheme 1). The prevalence of either bonding modes and, consequently, of either reaction path depends on both steric and electronic factors. In general, electron-rich metal fragments form η^2-*C,C* adducts, while sterically demanding fragments favor the η^1-*S* coordination mode.[5b,12e−f,16b,23] Since there is no reason at all to think of different steric crowding at the metal center in the isostructural fragments $[(triphos)RuH]^+$ and $[(triphos)RuH]^-$, a reasonable explanation for the observed selectivities is that both metal fragments react with BT to give equilibrium concentrations of η^1-*S* and η^2-*C,C* species whose evolution to products is kinetically controlled by hydride migration for Ru(II)) and by C−S insertion for Ru(0).

Whatever the intrinsic reasons for the different selectivity of BT hydrogenation catalyzed by $[(triphos)RuH]^+$ and $[(triphos)RuH]^-$ may be, it is a fact that the electron density at the metal center can, alone, influence the activation of the thiophene and ultimately be the driving force controlling the alternative hydrogenation → hydrogenolysis/ hydrogenolysis→ hydrogenation sequences in homogeneous phase (Scheme 1).

Differences and Commonalities Between Homogeneous and Heterogeneous Ru−Based HDS Catalysts. If the heterogeneous and homogeneous HDS reactions of thiophenes can indeed be related, the model study presented in this work provides some clues to unravel a number of mechanistic aspects of the HDS of thiophenes over single component Ru catalysts and eventually over Ru−Mo catalysts (it is generally agreed that the activation of thiophenes takes place at the promoter sites located at the MoS_2 edges, in fact).[1,25]

(21) Rhodes, L. F.; Sorato, C.; Venanzi, L. M.; Bachechi, F. *Inorg. Chem.* **1988**, *27*, 604.

(22) Bianchini, C.; Meli, A.; Vizza, F. Manuscript in preparation.

(23) (a) Robertson, M. J.; Day, C. L.; Jacobson, R. A.; Angelici, R. J. *Organometallics* **1994**, *13*, 179. (b) Choi, M.-G.; Angelici, R. J. *Organometallics* **1992**, *11*, 3328.

(24) (a) Sargent, A. L.; Titus, E. P. *Organometallics* **1998**, *17*, 65. (b) Myers, A. W.; Jones, W. D. *Organometallics* **1996**, *15*, 2905. (c) Myers, A. W.; Jones, W. D.; McClements, S. M. *J. Am. Chem. Soc.* **1995**, *117*, 11704. (d) Dong, L.; Duckett, S. B.; Ohman, K. F.; Jones, W. D. *J. Am. Chem. Soc.* **1992**, *114*, 151. (e) Jones, W. D.; Dong, L. *J. Am. Chem. Soc.* **1991**, *113*, 559.

(25) Startsev, A. N. *Catal. Rev.−Sci. Eng.* **1995**, *37*, 353.

The complexity of the reactions occurring during the HDS process reflects the chemical complexity of the catalyst surfaces over which the metal atoms active in promotion are capable of variable coordination numbers and variable oxidation states. A recent theoretical work by Harris illustrates remarkably this aspect for RuS_2 through the study of two-dimensional slabs exposing (210) and (111) surface planes.[2h] The electronic structure of 5-, 4-, and 3-coordinate Ru atoms has been related to the HDS activity, and the following conclusions have been forwarded. The 5-coordinate (210) surface site is suggested to be appropriate for coordinating thiophene but inappropriate for the C−S bond cleavage step, which conversely may take place at the more easily reducible 4-coordinate (210) Ru center. The 3-coordinate (111) Ru center, however, is the best candidate for the desulfurization step due to the high degree of coordinative unsaturation as well as the propensity to accept electron density from bulk Ru or H_2.

This heterogeneous scenario nicely fits the overall reactivity pattern exhibited by the "[(triphos)RuH]" system in the hydrogenation/hydrogenolysis of BT. In the +2 oxidation state of the metal, the coordination of BT is a facile process, but C−S insertion does not occur due to the lack of appropriate electron density at the 5-coordinate Ru(II) center. Once activated by coordination, BT is eventually hydrogenated to DHBT. In contrast, the C−S bond cleavage is a downhill process at the Ru(0) center in $[(triphos)RuH]^-$ and the hydrogenolysis reaction can readily take place under H_2.

The decreased HDS activity of heterogeneous catalysts upon addition of nitrogen compounds has been related to the existence of different metal sites on the surface.[1a,25,26,27] The presence of high-valent metal species capable of forming strong adducts with the N-donors (e.g. Ru(II) as shown here) may account for the decreased activity as the N-donor adducts on the surface may evolve to the hydrogen-resistant $(Ru)_3$-N, $(Ru)_2$-NH, or (Ru)-NH_2 moieties.[28] The residual activity of HDS catalysts poisoned with nitrogen donors may just be due to the presence of low-valent species which are more reluctant to bind the N-donors (e.g., Ru(0)) and thus less sensitive to deactivation. Consistently, we have found that the hydrogenolysis catalyst $[(triphos)RuH]^-$ does not coordinate MeCN, NH_3 or $NHEt_2$ and that the presence of nitrogen ligands in the catalytic mixture does not have any influence on the hydrogenolysis rate.[7]

In summary, the homogeneous studies suggest that the development of a new generation of effective and more robust Ru-based HDS catalysts may require one to increase the number of 3-coordinate surface Ru atoms as well as to apply a more efficient reducing environment.

As a final comment on the mechanistic relationships between heterogeneous and homogeneous HDS reactions of thiophenes, it is worth noticing that the removal of the sulfur products, ETP and DHBT, constitutes rate-limiting steps for both the hydrogenolysis and hydrogenation reactions of BT catalyzed by $[(triphos)RuH]^+$ and $[(triphos)RuH]^-$, respectively. To a certain extent, this finding witnesses the effectiveness of the "[(triphos)-RuH]" system in modeling the initial transformations of thiophenes over the surface of real HDS catalysts (Scheme 1) where the rate-determining step is commonly related to the rate of creation of sulfur vacancies.[1]

Conclusions

The $14e^-$ Ru(II) fragment $[(triphos)RuH]^+$, generated in situ by hydrogenation of $[(triphos)Ru(MeCN)_3]BPh_4$, is the most powerful catalyst for the selective conversion of BT to DHBT ever reported. With the use of this catalyst, the production of DHBT or of its 2,3-deuterated isotopomer is indeed available on any scale. The remarkable catalytic activities exhibited by $[(triphos)RuH]^+$ for the hydrogenation of BT to DHBT and by its $16e^-$ derivative $[(triphos)RuH]^-$ for the hydrogenolysis to ETP nicely fit the position of Ru-based heterogeneous catalysts in the periodic trends for HDS activity.[2] On the other hand, the system $[(triphos)RuH]^n$ ($n = -1, +1$) constitutes a valid model for mimicking the HDS activity of any single-component heterogeneous catalyst. In particular, a rationale for the concomitant occurrence of both hydrogenation and hydrogenolysis of thiophenes over heterogeneous catalysts has been forwarded in the light of the different chemoselectivity shown by the $[(triphos)RuH]^+$ and $[(triphos)RuH]^-$ catalysts in the hydrogenation of BT. The interaction of these catalysts with some nitrogen and oxygen compounds, particularly ammonia and water, has been studied in an attempt to rationalize the facile deactivation of Ru catalysts in actual HDS conditions during which nitrogen and oxygen compounds may be produced by the concomitant hydrodenitrogenation (HDN) and hydrodeoxygenation (HDO) processes.[1] The results obtained from our investigation have outlined the potential of homogeneous modeling studies for getting insight into the deactivation of HDS catalysts which is probably one of the areas where a more detailed understanding will have a large industrial impact in the future.

Acknowledgment. A contract (PR1/C) from the Ministero dell'Ambiente of Italy, a project (S1-95000693) from CONICIT (Venezuela), and a cooperation agreement between the CNR (Italy) and CONICIT (Venezuela) are gratefully acknowledged for financial support.

Supporting Information Available: Kinetic (Figures 3−5,7) and Arrhenius (Figure 6) plots for the hydrogenation of BT to DHBT with **1** as catalyst precursor. This material is available free of charge via the Internet at http://pubs.acs.org.

JA983224E

(26) (a) LaVopa, V.; Satterfield, C. N. *J. Catal.* **1988**, *110*, 375. (b) Nagai, M.; Sato, T.; Aiba, A. *J. Catal.* **1986**, *97*, 52. (c) Nagai, M.; Kabe, T. *J. Catal*. **1983**, *81*, 440. (d) Ramachandran, R.; Massoth, F. E. *Chem. Eng. Commun.* **1982**, *18*, 239. (e) Lee, H. C.; Butt, J. B. *J. Catal.* **1977**, *49*, 320.

(27) Amberg, C. H. *J. Less-Common Met.* **1974**, *36*, 339.

(28) (a) Ho, T. C. *Catal. Rev.−Sci. Eng.* **1988**, *30*, 117. (b) Katzer, J. R.; Sivasubramanian, R. *Catal. Rev.−Sci. Eng.* **1979**, *20*, 155.